Stapled Peptides Hot Paper

DOI: 10.1002/anie.201308568

Direct Targeting of Rab-GTPase–Effector Interactions**

Jochen Spiegel, Philipp M. Cromm, Aymelt Itzen, Roger S. Goody, Tom N. Grossmann, and Herbert Waldmann**

Abstract: *Small GTPases are molecular switches using GDP/GTP alternation to control numerous vital cellular processes. Although aberrant function and regulation of GTPases are implicated in various human diseases, direct targeting of this class of proteins has proven difficult, as GTPase signaling and regulation is mediated by extensive and shallow protein interfaces. Here we report the development of inhibitors of protein–protein interactions involving Rab proteins, a subfamily of GTPases, which are key regulators of vesicular transport. Hydrocarbon-stapled peptides were designed based on crystal structures of Rab proteins bound to their interaction partners. These modified peptides exhibit significantly increased affinities and include a stapled peptide (StRIP3) that selectively binds to activated Rab8a and inhibits a Rab8a–effector interaction in vitro.*

Small GTPases are involved in a variety of pivotal cellular processes including cell growth, differentiation and survival, vesicular transport, and membrane trafficking.[1] These switch molecules alternate between an inactive GDP-bound and an active GTP-bound form. Their activity and subsequent signal propagation are regulated by protein–protein interactions (PPIs), including binding to guanine nucleotide exchange factors (GEFs) and GTPase activating proteins (GAPs). GEFs stabilize the nucleotide-free state (NF) thereby catalyzing nucleotide exchange from GDP to GTP. GAPs recognize GTP-bound forms and enhance the intrinsically low GTPase activity.[2,3] Switching between nucleotide binding states involves major conformational changes and allows activated GTPases to specifically interact with different effector proteins thereby triggering downstream signaling events. Aberrant activation of small GTPases is implicated in numerous human diseases, rendering members of this protein family very attractive targets in drug discovery.[4] For instance, Rab (Ras-related in brain) proteins are master regulators of intracellular vesicular transport and trafficking, and malfunctions of Rab GTPases have been implicated in an increasing number of inherited and acquired pathologies including neurodegenerative diseases and various forms of cancer.[5]

In general, interfering with GTPase activity and function has proven to be very difficult. In particular, direct modulation of protein–protein interactions involving GTPases is a major challenge,[6] since the corresponding protein interfaces lack well-defined binding pockets. Only in a few cases modulators of small GTPase–protein interactions were reported,[7] most of them targeting Ras proteins[8] with a focus on Ras–GEF interactions.[9] Compounds directly targeting Rab GTPases have not been described so far. Stabilized helical peptides have been successfully employed to target PPIs that are very hard to address by small molecules.[10] Here we report the inhibition of PPIs involving Rab8 as a representative GTPase using helical peptides derived from α-helical binding motifs of Rab-interacting proteins that were stabilized by means of hydrocarbon–peptide stapling.[11]

In order to identify peptide sequences suitable to serve as a starting point for the design of Rab-PPI inhibitors, we analyzed known crystal structures of Rab in complex with protein binding partners and searched for cases in which binding to Rab is mediated by α-helical interaction motifs suitable to initiate a peptide-stapling approach (Figure 1 a and Figure S1).[3] To evaluate whether the corresponding α-helical peptides might retain the potential for Rab binding, we calculated their interaction surface with the Rab protein based on available structural data. Using the Protein Data Bank (http://www.pdb.org)[12] as a source, we identified nine

[*] J. Spiegel,[+] P. M. Cromm,[+] Dr. T. N. Grossmann, Prof. Dr. H. Waldmann
Max-Planck-Institut für Molekulare Physiologie
Abteilung Chemische Biologie
Otto-Hahn-Strasse 11, 44227 Dortmund (Germany)
and
Technische Universität Dortmund
Fakultät für Chemie und Chemische Biologie
Otto-Hahn-Strasse 6, 44227 Dortmund (Germany)
E-mail: tom.grossmann@mpi-dortmund.mpg.de
herbert.waldmann@mpi-dortmund.mpg.de

Prof. Dr. A. Itzen
Center for Integrated Protein Science Munich
Chemistry Department, Technische Universität München
Lichtenbergstrasse 4, 85748 Garching (Germany)

Prof. Dr. R. S. Goody
Max-Planck-Institut für Molekulare Physiologie
Abteilung Physikalische Biochemie
Otto-Hahn-Strasse 11, 44227 Dortmund (Germany)

Dr. T. N. Grossmann
Chemical Genomics Centre of the Max Planck Society
Otto-Hahn-Strasse 15, 44227 Dortmund (Germany)

[+] These authors contributed equally to this work.

[**] This work was funded by the European Research Council under the European Union's Seventh Framework Programme (FP7/2007-2013) (ERC Grant No. 268309). T.N.G and J.S. acknowledge financial support by the Fonds der Chemischen Industrie. P.M.C. is thankful to the Studienstiftung des deutschen Volkes for a fellowship. We thank N. Bleiming for protein expression/purification and technical assistance. The Dortmund Protein Facility is acknowledged for assistance in cloning and protein expression and purification.

Supporting information for this article is available on the WWW under http://dx.doi.org/10.1002/anie.201308568.

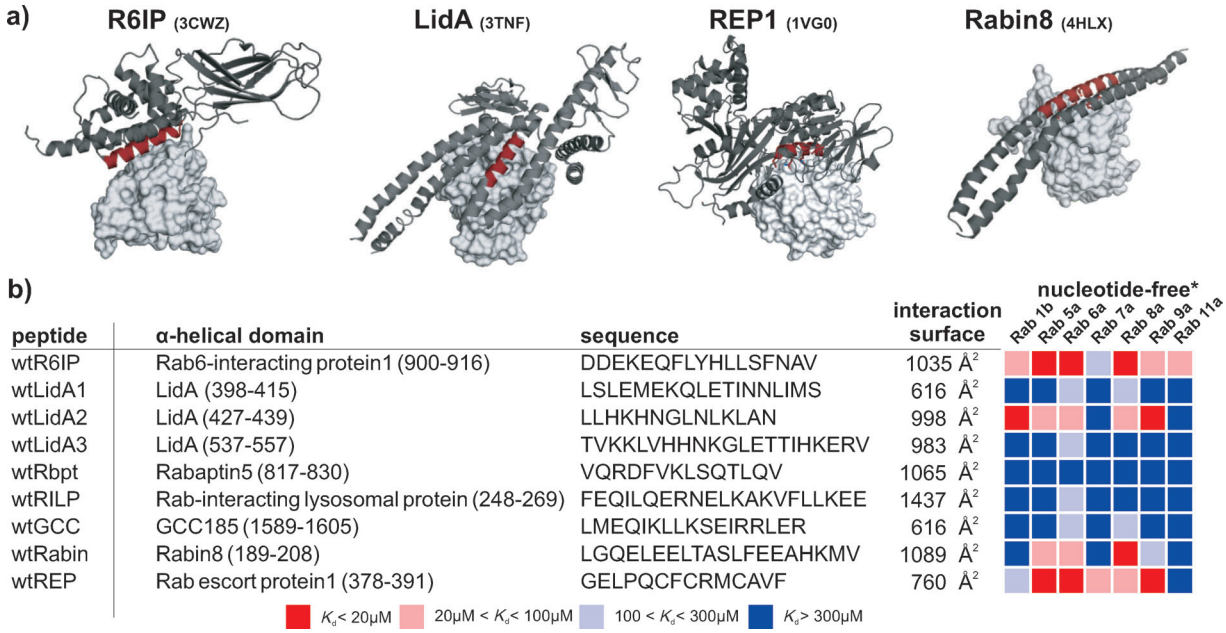

Figure 1. Helical interaction motifs of Rab binding partners. a) Crystal structures of Rab proteins and their natural ligands. Helices involved in the binding interface and used for further modification are highlighted in red. b) Synthesized wild-type peptides with their parent protein, corresponding interaction surface, and a heatmap representation of the dissociation constants observed with different nucleotide-free Rab proteins. * Nucleotide-free Rab proteins generally suffer from poor solubility resulting in relatively low final protein concentrations (maximum concentration in FP: Rab1b(NF) = 105 μM, Rab5a(NF) = 4 μM, Rab6a(NF) = 140 μM, Rab7a(NF) = 57 μM, Rab8a(NF) = 34 μM, Rab9a(NF) = 5 μM, Rab11a(NF) = 171 μM). As a consequence, some of the binding curves do not reach a plateau and are extrapolated in order to obtain comparable K_d values (for details see Tables S4–S6 and Figures S7–S13).

candidates originating from different effector and regulatory proteins that bury at least 600 Å^2 of solvent-accessible surface area (Figure 1b and Table S1).[13] These peptides were synthesized as N-terminal fluorescein–PEG conjugates by Fmoc-based solid-phase peptide synthesis (SPPS) (see Table S2).

Since most of the parent proteins bind multiple Rab GTPases, we assessed the affinity of the nine peptides to a representative set of Rab proteins (Rab1b/-5a/-6a/-7a/-8a/-9a/-11a) using a fluorescence polarization (FP) assay. The nucleotide binding state of the Rab proteins dictates their affinity to corresponding binding partners, with effector proteins such as Rab6-interacting protein1, LidA, Rabaptin5, Rab-interacting lysosomal protein, and GCC185 preferably binding to the activated GTP-bound form. GEFs such as Rabin8 show the highest affinity for the nucleotide-free form, whereas Rab escort protein1 preferentially binds to GDP-bound Rab proteins. Therefore, all Rab proteins were generated in the three nucleotide binding states (GDP, GTP, nucleotide-free) and investigated using FP. Except in the case of Rab6a,[14] which is maintained in the GTP state due to an exceptionally low intrinsic GTPase activity, the nonhydrolyzable GTP analogue GppNHp was used to avoid intrinsic hydrolysis. All tested peptides displayed low affinities (dissociation constant: $K_d > 300$ μM) for nucleotide-bound Rab proteins, which is not surprising since the α-helical fragments presumably lose their secondary structure when excised from the corresponding parent protein. However, four of the nine peptides (wtR6IP, wtLidA2, wtRabin8, and wtREP) exhibited dissociation constants with nucleotide-free Rab proteins in the low to medium micromolar range (Figure 1b and Tables S4–S6). Discrimination between the different Rab proteins by these peptides is relatively low, possibly because the excised α-helical domains represent only a part of the original binding interface. In addition, nucleotide-free Rab proteins exhibit an increased degree of flexibility in proximity to the nucleotide-binding regions which might support induced-fit binding.

From the established approaches to stabilizing and thereby restoring the binding affinity of small α-helical peptides, we applied hydrocarbon–peptide stapling, which has proven very useful for targeting protein–protein interactions.[11] Peptide stapling requires the introduction of α-methyl, α-alkenyl amino acids into a peptide sequence and subsequent macrocycle formation to generate an all-hydrocarbon bridge connecting two turns of an α-helix. In its most successful realization, two *S*-configured modified amino acids incorporated at positions i and $i+4$ are used to form an eight-carbon cross-link (Figure 2a and b)[15] which may result in an increase of target affinity in the range of one to two orders of magnitude. The four peptides (wtR6IP, wtLidA2, wtRabin8, and wtREP) with low micromolar affinity for nucleotide-free Rabs were chosen for stapling.

Based on crystal structures of the parent protein–Rab complexes, residues that do not contribute to Rab binding were identified for staple incorporation. For instance, the Rab6a(GTP)–Rab6 interacting protein1 complex (PDB 3CWZ; Figure 2c) reveals five potential modification sites (gray spheres, Figure 2d) for which we identified three positions for incorporation of $i,i+4$ hydrocarbon staples

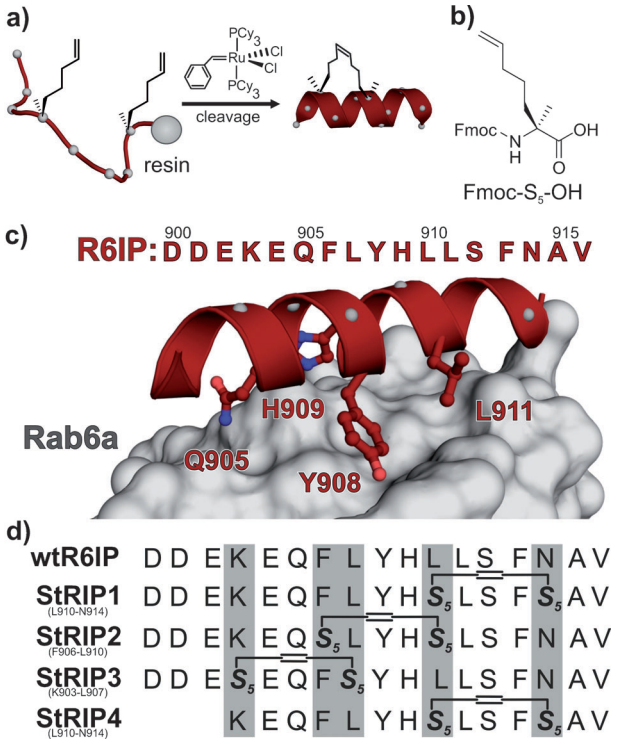

Figure 2. Design of stapled peptides derived from Rab6-interacting protein1. a) The peptide-stapling approach: The α-methyl, α-alkenyl building block Fmoc-S_5-OH (see (b)) is incorporated into the peptide sequence at positions *i* and *i*+4 and cross-linked by ring-closing olefin metathesis. (For detailed information on the syntheses of the building blocks and the peptides see Figures S5 and S6.) c) Crystal structure of Rab6-interacting protein1 (R6IP) bound to Rab6a (PDB 3CWZ). Side chains involved in the binding are shown explicitly and residues selected for introduction of Fmoc-S_5-OH are highlighted as gray spheres. d) Sequences of the four stapled peptides derived from R6IP.

(StRIP1-3). In addition, a shorter stapled peptide (StRIP4) was designed to investigate the importance of the negatively charged N-terminus. For peptide stapling implementing the *i*,*i*+4 cross-link, the nonnatural amino acid Fmoc-S_5-OH (Fmoc-(*S*)-2-amino-2-methyl-hept-6-enoic acid, Figure 2b and Figure S5) was introduced into the peptide sequence during SPPS and subsequently the side chains were cross-linked using ruthenium-mediated olefin metathesis. Finally, the N-terminus was either fluorescently labeled as described above or acetylated using acetic anhydride (see Table S3).

In analogy to the stabilized derivatives of wtR6IP, stapled peptides were designed using wtLidA2, wtRabin8, and wtREP as starting points (Figure 3a and Figures S2–S4). Three stapled peptides StLidA1–3 were generated based on the Rab8a(GppNHp)–LidA crystal structure (PDB 3TNF). Although we identified three different stapling patterns in the Rab7(GDP)–Rab escort protein1 complex (PDB 1VG0), only two of them were synthetically accessible, probably due to the helix-breaking properties of proline 381. For the slightly longer wtRabin sequence, four different stapled peptides (StRabin1–4) were obtained based on the Rab8(NF)–Rabin8 complex (PDB 4HLX). Subsequently, all stapled peptides were investigated by means of circular dichroism (CD) spectroscopy. In most cases α-helicity was increased compared to that of the unmodified starting sequences, with StRIP1 (36%) and StRabin1 (35%) exhibiting the highest α-helicity (Figure 3a and b, Table S8, and Figure S32).[16]

The affinities of the fluorescein-labeled stapled peptides were determined for Rab1b/-5a/-6a/-8a/-9a/-11a each in the three nucleotide binding states using FP (Figure 3a,c; Table S6 and Figures S14–S31). For nucleotide-free Rab proteins almost all stapled analogues showed increased binding affinities compared to those of the corresponding wild-type peptides (up to 200-fold). Only stapled peptides StLidA2 (for Rab9a(NF) and Rab11a(NF)) and StLidA3 (for all tested Rab(NF) proteins) did not show improved binding. For Rab8a(NF) and Rab11a(NF) several ligands displayed dissociation constants in the submicromolar range, with StRIP3/Rab11 [$K_d = (0.40 \pm 0.02)$ μM] and StREP2/Rab8a [$K_d = (0.42 \pm 0.03)$ μM] exhibiting the highest affinity. The dissociation constants of the best binders for Rab1b, -5a, and -6a in their nucleotide-free form were determined to be between 1.0 μM and 1.1 μM with a maximum increase in affinity of 40-fold as a result of stapling. Only for Rab9(NF) were K_d values determined to be above 10 μM. Similar to the wild-type sequences, the investigated stapled peptides show low discrimination between different Rab proteins. However, the stapled peptides exhibit low affinity ($K_d > 100$ μM) for the GDP-bound and most of the GTP-/GppNHp-bound Rab proteins which reflects the low affinity of the starting wild-type sequences. Nevertheless, several peptides bind Rab8a in its GppNHp-bound state. Six stapled peptides exhibited moderate K_d values in the range of 50 μM to 100 μM. Most strikingly, the stabilized α-helical domain of Rab6 interacting protein1, StRIP3, bound Rab8a(GppNHp) with a K_d of (22.2 ± 1.2) μM, which is in the range of some effector proteins.[17,18] Moreover, StRIP3 demonstrated an at least fivefold selectivity for Rab8a(GppNHp) over the other tested Rab proteins. Notably, StRIP3 is the first identified low-micromolar binder of a Rab GTPase in its activated GTP-bound form.

To explore the contributions of the introduced staple to binding, we synthesized StRIP3 derivatives with longer and shorter linkers. This resulted in peptides with reduced affinities for Rab8(GppNHp) (Figures S33 and S34). Additionally, the starting sequence of StRIP3 (wtR6IP) was stabilized using an N-terminal hydrogen-bond surrogate (HBS).[19] The affinity of the HBS-stabilized helix was twice that of wtR6IP but did not reach the ninefold improvement observed for StRIP3 (see Figures S32 and S34). Furthermore, we varied the central amino acid sequence and therefore replaced leucine 911 (Figure 2c) with amino acids carrying side chains of different steric demand and polarity (Figure S33 and S34). The modifications did not yield peptides with significantly increased affinities.

For active compounds it is important that they are able to bind their target in a complex protein mixture. Therefore, we tested the most affine stapled peptide StRIP3 regarding its ability to bind Rab8 in the context of a cellular lysate. We performed affinity isolation (pull-down) assays using HCT116 lysates enriched with 0.9 wt% Rab8(GppNHp) (based on protein content). The stapled peptide StRIP3 and the weaker

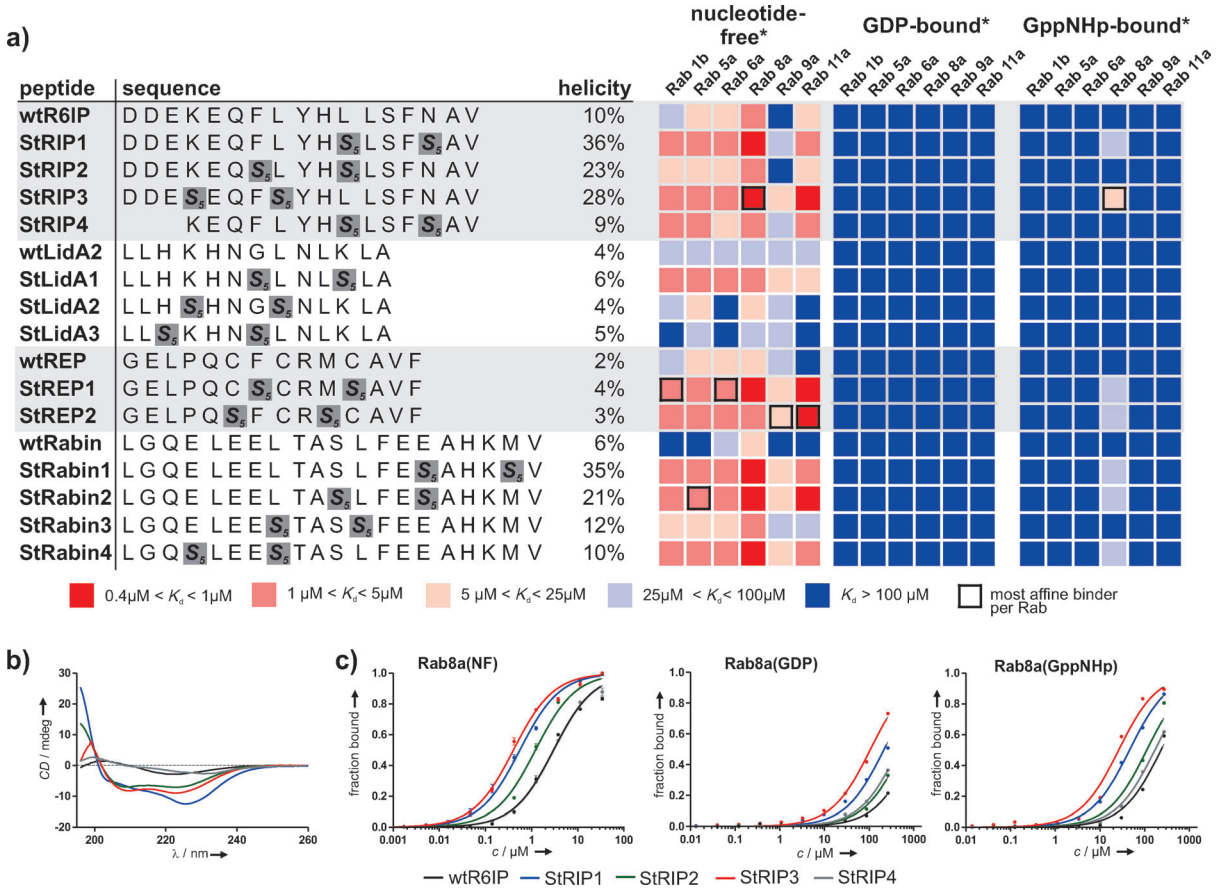

Figure 3. Evaluation of stapled peptides: a) Hydrocarbon-stapled peptide sequences, α-helicity, and heatmap representation of the dissociation constants of the FITC-labeled peptides with different Rab proteins in all three nucleotide binding states. * Maximum employed protein concentrations were c_{max}[Rab1b(NF)] = 110 μM, c_{max}[Rab5a(NF)] = 5 μM, c_{max}[Rab6a(NF)] = 100 μM, c_{max}[Rab8a(NF)] = 34 μM, c_{max}[Rab9a(NF)] = 68 μM, and c_{max}[Rab11a(NF] = 170 μM; nucleotide-free forms were employed close to their solubility limit; c_{max}[Rab(GDP)] = 300 μM and c_{max}[Rab(GppNHp)] = 300 μM. FP data and explicit dissociation constants as well as detailed information on CD and K_d calculation are provided in Table S6 and Figures S14–S31. b) Representative CD spectra of acetylated StRIP peptides. c) Representative FP binding data of FITC-labeled StRIP peptides with Rab8a.

ligand wtR6IP were labeled with biotin and immobilized on streptavidin beads which subsequently were incubated with Rab8(GppNHp)-enriched cellular lysate. Western blotting analysis with Rab8a-specific antibodies clearly showed that pull-down efficiency correlated well with the binding profile determined in the FP assay (Figure 4a). To explore its functional activity, we were finally interested in the ability of StRIP3 to compete with Rab8 effector binding. We chose the Rab8a effector oculocerebrorenal syndrome of Lowe (Lowe syndrome) protein (OCRL1), a peripheral membrane protein mainly located at the Golgi apparatus, for further studies. Mutations of OCRL1 are implicated in the initiation and progression of Lowe syndrome.[20] The Rab8-binding domain of OCRL1 (amino acids 539–901) was labeled with a N-hydroxysuccinimide-fluorescein conjugate and binding to Rab8a(GppNHp) was monitored by means of FP. The observed dissociation constant of 1.7 μM for $OCRL1_{539-901}$ and Rab8a(GppNHp) (see Figure S36) correlates well with the reported affinity[17] (K_d = 0.9 μM) for unmodified $OCRL1_{539-901}$. To investigate the ability of StRIP3 to disrupt this interaction, competition FP experiments were performed. In this assay, concentration-dependent displacement of labeled $OCRL1_{539-901}$ by acetylated StRIP3 was observed whereas control peptides StRIP4 and wtR6IP did not interfere with OCRL1 binding (Figure 4b). For inhibition of the Rab8a(GppNHp)–$OCRL1_{539-901}$ complex formation by StRIP3 an IC_{50} of (490 ± 65) μM was determined. The titration curve obtained in this experiment could be well explained using a purely competitive model and assuming a K_d value for the StRIP3 peptide of roughly 45 μM. Simulation of the

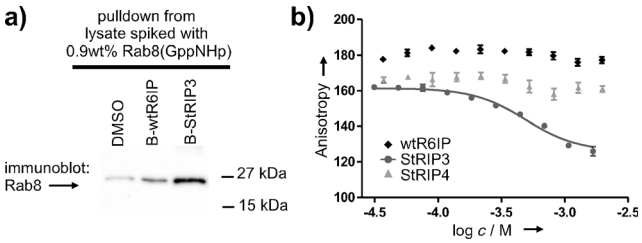

Figure 4. In vitro characterization of StRIP3: a) Pulldown assay with biotinylated peptides in spiked HCT116 lysate. b) Displacement titration of fluorescein-labeled $ORCL1_{539-901}$ (50 nM) from Rab8a(GppNHp) (10 μM) with increasing concentrations of acetylated StRIP3.

binding curve using the program Scientist (Micromath) gave a calculated IC_{50} value of about 0.5 mM, in good agreement with the experimental value. Although the K_d value is roughly twice that obtained by direct titration of the peptide with Rab8a, this is in reasonable agreement in view of the different procedures used and can be taken as support for the direct competitive inhibition of binding of the effector OCRL1 to Rab8a by StRIP3. A more extensive analysis would be needed to determine the exact nature of the binding (i.e. whether the binding is purely or possibly partially competitive).

Interactions between Rab GTPases and their protein binding partners involve extensive, shallow surfaces, preventing the application of most conventional targeting approaches. Due to their involvement in the pathogenesis of various human diseases, several Rab proteins have recently emerged as new therapeutic targets. However, compounds directly targeting Rab GTPases and, in particular PPIs involving Rabs, have not been reported up to this point. Here we report that protein–protein interactions involving Rab GTPases—and in extension possibly other GTPases as well—can successfully be targeted using hydrocarbon-stapled peptides. A set of α-helical interaction motifs was identified, stabilized, and investigated for binding to several Rab proteins in their three nucleotide binding states. Insertion of an all-hydrocarbon staple into the α-helical binding motifs increased the affinity of the peptide ligand for Rab proteins in almost all cases resulting in more than 200-fold higher binding affinity compared to the parent peptides. The most potent peptide displayed a K_d of 0.4 μM with Rab proteins in their nucleotide-free from. Notably, a stapled peptide (StRIP3) was identified which selectively binds to Rab8a in its activated GppNHp-bound state, exhibiting an affinity comparable to that of Rab effector proteins. StRIP3 displays functional activity in vitro by competing with a Rab8a–effector interaction. This peptide represents the first compound directly targeting Rab GTPases and inhibiting Rab–protein interactions. Given the fact that direct targeting of small GTPases for a modulation of effector binding has proven extremely difficult, our strategy might represent a novel path to successfully overcome this obstacle.

Received: October 1, 2013
Revised: November 26, 2013
Published online: January 31, 2014

Keywords: inhibitors · protein–protein interactions · Rab proteins · stapled peptides

[1] a) H. R. Bourne, D. A. Sanders, F. McCormick, *Nature* **1990**, *348*, 125 – 132; b) J. Cherfils, M. Zeghouf, *Physiol. Rev.* **2013**, *93*, 269 – 309.

[2] A. Itzen, R. S. Goody, *Semin. Cell Dev. Biol.* **2011**, *22*, 48 – 56.

[3] A. H. Hutagalung, P. J. Novick, *Physiol. Rev.* **2011**, *91*, 119 – 149.

[4] a) R. S. Bon, Z. Guo, E. A. Stigter, S. Wetzel, S. Menninger, A. Wolf, A. Choidas, K. Alexandrov, W. Blankenfeldt, R. S. Goody, et al., *Angew. Chem.* **2011**, *123*, 5059 – 5063; *Angew. Chem. Int. Ed.* **2011**, *50*, 4957 – 4961; b) N. Berndt, A. D. Hamilton, S. M. Sebti, *Nat. Rev. Cancer* **2011**, *11*, 775 – 791; c) E. A. Stigter, Z. Guo, R. S. Bon, Y.-W. Wu, A. Choidas, A. Wolf, S. Menninger, H. Waldmann, W. Blankenfeldt, R. S. Goody, *J. Med. Chem.* **2012**, *55*, 8330 – 8340; d) G. Zimmermann, B. Papke, S. Ismail, N. Vartak, A. Chandra, M. Hoffmann, S. A. Hahn, G. Triola, A. Wittinghofer, P. I. H. Bastiaens, et al., *Nature* **2013**, *497*, 638 – 642.

[5] a) S. Mitra, K. W. Cheng, G. B. Mills, *Semin. Cell Dev. Biol.* **2011**, *22*, 57 – 68; b) J. O. Agola, P. A. Jim, H. H. Ward, S. Basuray, A. Wandinger-Ness, *Clin. Genet.* **2011**, *80*, 305 – 318.

[6] G. L. Verdine, L. D. Walensky, *Clin. Cancer Res.* **2007**, *13*, 7264 – 7270.

[7] a) L. Renault, B. Guibert, J. Cherfils, *Nature* **2003**, *426*, 525 – 530; b) M. Hafner, A. Schmitz, I. Grüne, S. G. Srivatsan, B. Paul, W. Kolanus, T. Quast, E. Kremmer, I. Bauer, M. Famulok, *Nature* **2006**, *444*, 941 – 944; c) Q. Zhang, M. B. Major, S. Takanashi, N. D. Camp, N. Nishiya, E. C. Peters, M. H. Ginsberg, X. Jian, P. A. Randazzo, P. G. Schultz, et al., *Proc. Natl. Acad. Sci. USA* **2007**, *104*, 7444 – 7448; d) J. Viaud, M. Zeghouf, H. Barelli, J.-C. Zeeh, A. Padilla, B. Guibert, P. Chardin, C. A. Royer, J. Cherfils, A. Chavanieu, *Proc. Natl. Acad. Sci. USA* **2007**, *104*, 10370 – 10375; e) L. Hong, S. R. Kenney, G. K. Phillips, D. Simpson, C. E. Schroeder, J. Noth, E. Romero, S. Swanson, A. Waller, J. J. Strouse, et al., *J. Biol. Chem.* **2013**, *288*, 8531 – 8543.

[8] a) C. Herrmann, C. Block, C. Geisen, K. Haas, C. Weber, G. Winde, T. Möröy, O. Müller, *Oncogene* **1998**, *17*, 1769 – 1776; b) J. Kato-Stankiewicz, I. Hakimi, G. Zhi, J. Zhang, I. Serebriiskii, L. Guo, H. Edamatsu, H. Koide, S. Menon, R. Eckl, et al., *Proc. Natl. Acad. Sci. USA* **2002**, *99*, 14398 – 14403; c) P. C. Gareiss, A. R. Schneekloth, M. J. Salcius, S.-Y. Seo, C. M. Crews, *ChemBioChem* **2010**, *11*, 517 – 522; d) I. C. Rosnizeck, M. Spoerner, T. Harsch, S. Kreitner, D. Filchtinski, C. Herrmann, D. Engel, B. König, H. R. Kalbitzer, *Angew. Chem.* **2012**, *124*, 10799 – 10804; *Angew. Chem. Int. Ed.* **2012**, *51*, 10647 – 10651; e) F. Shima, Y. Yoshikawa, M. Ye, M. Araki, S. Matsumoto, J. Liao, L. Hu, T. Sugimoto, Y. Ijiri, A. Takeda, et al., *Proc. Natl. Acad. Sci. USA* **2013**, *110*, 8182 – 8187.

[9] a) A. K. Ganguly, Y.-S. Wang, B. N. Pramanik, R. J. Doll, M. E. Snow, A. G. Taveras, S. Remiszewski, D. Cesarz, J. del Rosario, B. Vibulbhan, et al., *Biochemistry* **1998**, *37*, 15631 – 15637; b) A. Patgiri, K. K. Yadav, P. S. Arora, D. Bar-Sagi, *Nat. Chem. Biol.* **2011**, *7*, 585 – 587; c) Q. Sun, J. P. Burke, J. Phan, M. C. Burns, E. T. Olejniczak, A. G. Waterson, T. Lee, O. W. Rossanese, S. W. Fesik, *Angew. Chem.* **2012**, *124*, 6244 – 6247; *Angew. Chem. Int. Ed.* **2012**, *51*, 6140 – 6143; d) T. Maurer, L. S. Garrenton, A. Oh, K. Pitts, D. J. Anderson, N. J. Skelton, B. P. Fauber, B. Pan, S. Malek, D. Stokoe, et al., *Proc. Natl. Acad. Sci. USA* **2012**, *109*, 5299 – 5304.

[10] a) J. Garner, M. M. Harding, *Org. Biomol. Chem.* **2007**, *5*, 3577 – 3585; b) L. K. Henchey, A. L. Jochim, P. S. Arora, *Curr. Opin. Chem. Biol.* **2008**, *12*, 692 – 697; c) M. Raj, B. N. Bullock, P. S. Arora, *Bioorg. Med. Chem.* **2013**, *21*, 4051 – 4057; d) R. Dharanipragada, *Future Med. Chem.* **2013**, *5*, 831 – 849; e) V. Azzarito, K. Long, N. S. Murphy, A. J. Wilson, *Nat. Chem.* **2013**, *5*, 161 – 173.

[11] a) C. E. Schafmeister, J. Po, G. L. Verdine, *J. Am. Chem. Soc.* **2000**, *122*, 5891 – 5892; b) L. D. Walensky, A. L. Kung, I. Escher, T. J. Malia, S. Barbuto, R. D. Wright, G. Wagner, G. L. Verdine, S. J. Korsmeyer, *Science* **2004**, *305*, 1466 – 1470; c) E. Gavathiotis, M. Suzuki, M. L. Davis, K. Pitter, G. H. Bird, S. G. Katz, H.-C. Tu, H. Kim, E. H.-Y. Cheng, N. Tjandra, et al., *Nature* **2008**, *455*, 1076 – 1081; d) R. E. Moellering, M. Cornejo, T. N. Davis, C. D. Bianco, J. C. Aster, S. C. Blacklow, A. L. Kung, D. G. Gilliland, G. L. Verdine, J. E. Bradner, *Nature* **2009**, *462*, 182 – 188; e) G. H. Bird, N. Madani, A. F. Perry, A. M. Princiotto, J. G. Supko, X. He, E. Gavathiotis, J. G. Sodroski, L. D. Walensky, *Proc. Natl. Acad. Sci. USA* **2010**, *107*, 14093 – 14098; f) M. L. Stewart, E. Fire, A. E. Keating, L. D. Walensky, *Nat. Chem. Biol.*

2010, *6*, 595 – 601; g) T. N. Grossmann, J. T.-H. Yeh, B. R. Bowman, Q. Chu, R. E. Moellering, G. L. Verdine, *Proc. Natl. Acad. Sci. USA* **2012**, *109*, 17942 – 17947; h) Y. S. Chang, B. Graves, V. Guerlavais, C. Tovar, K. Packman, K.-H. To, K. A. Olson, K. Kesavan, P. Gangurde, A. Mukherjee, et al., *Proc. Natl. Acad. Sci. USA* **2013**, *110*, E3445 – E3454; i) W. Kim, G. H. Bird, T. Neff, G. Guo, M. A. Kerenyi, L. D. Walensky, S. H. Orkin, *Nat. Chem. Biol.* **2013**, *9*, 643 – 650.

[12] H. M. Berman, J. Westbrook, Z. Feng, G. Gilliland, T. N. Bhat, H. Weissig, I. N. Shindyalov, P. E. Bourne, *Nucleic Acids Res.* **2000**, *28*, 235 – 242.

[13] M. F. Sanner, A. J. Olson, J.-C. Spehner, *Biopolymers* **1996**, *38*, 305 – 320.

[14] T. Bergbrede, O. Pylypenko, A. Rak, K. Alexandrov, *J. Struct. Biol.* **2005**, *152*, 235 – 238.

[15] Y.-W. Kim, T. N. Grossmann, G. L. Verdine, *Nat. Protoc.* **2011**, *6*, 761 – 771.

[16] Extending the length of the synthesized helix is expected to improve helicity and affinity as observed for StRIP4/StRIP1 (Figure 3a) and StRabin1/StRabin1 XL (Table S9). However, StRIP3, StLidA, and StREP already contain the complete helical binding domain according to the corresponding crystal structures (PDB: 3CWZ, 3TNF, and 1VG0).

[17] A. S. Burguete, T. D. Fenn, A. T. Brunger, S. R. Pfeffer, *Cell* **2008**, *132*, 286 – 298.

[18] X. Hou, N. Hagemann, S. Schoebel, W. Blankenfeldt, R. S. Goody, K. S. Erdmann, A. Itzen, *EMBO J.* **2011**, *30*, 1659 – 1670.

[19] A. Patgiri, A. L. Jochim, P. S. Arora, *Acc. Chem. Res.* **2008**, *41*, 1289 – 1300.

[20] O. Attree, I. M. Olivos, I. Okabe, L. C. Bailey, D. L. Nelson, R. A. Lewis, R. R. Mclnnes, R. L. Nussbaum, *Nature* **1992**, *358*, 239 – 242.

